Rare earth–cobalt hard magnetic nanoparticles and nanoflakes by high-energy milling

A M Gabay[1]**, N G Akdogan**[1]**, M Marinescu**[2]**, J F Liu**[2] **and**
G C Hadjipanayis[1]

[1] Department of Physics and Astronomy, University of Delaware, Newark, DE 19716, USA
[2] Electron Energy Corporation, Landisville, PA 17538, USA

E-mail: gabay@physics.udel.edu

Abstract
High-energy ball milling has been shown to be a promising method for large-scale fabrication of rare earth–transition metal nanoparticles. In this work, we report crystallographically anisotropic $SmCo_5$, $PrCo_5$ and $Sm_2(Co, Fe)_{17}$ nanoparticles (particle size smaller than 10 nm) obtained by surfactant-assisted ball milling and study their size and properties as a function of the milling conditions. By milling nanocrystalline precursor alloys, we obtained $SmCo_5$ platelets (flakes) approximately 100 nm thick with an aspect ratio as high as 10^2–10^3. The unusual shape evolution of this brittle material is attributed to its increased plasticity in the nanocrystalline state. The nanoflakes are susceptible to re-crystallization annealing and exhibit a room-temperature coercivity of up to 19 kOe. The successful fabrication of rare earth–cobalt nanoparticles and ultra-thin flakes provides hope for the development of nanocomposite permanent magnets with an enhanced energy product.

1. Introduction

Recent years saw increasing demand for even finer permanent magnet powders based on rare earth–transition metal (RE–TM) compounds. The potential applications of hard magnetic powders consisting of particles ranging from a few to a hundred nanometers stretch from nanocomposite magnets with superior magnetic energy storage capacity [1, 2] to microelectromechanical systems [3]. However, fabrication of ultra-fine powders from these highly reactive materials has always been very challenging. Submicron- and nanoparticles of the RE–TM compounds exhibiting a moderately high coercivity were produced via a short-pulse electrodeposition technique [4] and spark erosion [5–7]. The most comprehensive and promising results reported to date have been obtained via various ball-milling techniques: hydrogenation-assisted milling [8, 9], thermomechanical synthesis [10, 11], dry milling in argon [12, 13] and especially wet milling in organic solvents in the presence of surfactants [14–18]. This paper, which elaborates on the latter approach, reports the fabrication of crystallographically anisotropic $SmCo_5$, $PrCo_5$ and Sm_2Co_{17} nanoparticles.

Milling in the presence of a fluid and/or surfactants is known to decrease particle agglomeration during milling [19, 20]; other effects also include the lowering of energies of freshly cleaved surfaces, enabling long-range capillary forces (and therefore lowering the energy required for crack propagation), and decrease inter-particle friction [21]. It usually takes a very long time to obtain nanoparticles with *low-energy* surfactant-assisted ball milling [22]; therefore the *high-energy* ball milling (HEBM) is typically used when dealing with materials as reactive as RE–TM.

Use of surfactants during ball milling is known to influence not only the size of the particles, but also their shape. In the case of ductile or, more exactly, malleable metals and alloys, the shape of ball-milled particles can be controlled by varying the milling environment. Dry milling yields more or less equiaxed particles [23], whereas wet milling, particularly with a high-energy mill and/or at a high ball-to-powder ratio, results in high-aspect-ratio flakes, often with a submicron thickness [23–27]. According to [26], copper powder is significantly more susceptible to the 'flaking' during milling than nickel powder. This difference underlines the critical role of malleability (rather than ductility) in the particle

shape evolution: copper is more malleable but less ductile than nickel. The RE–TM hard magnetic materials are inherently brittle and, therefore, should not be susceptible to 'flaking'. However, even brittle materials may exhibit a significant ductility if they have a nanocrystalline structure [28]. It has been shown [29, 30] that dry high-energy ball milling (HEBM) of RE–Co alloys is very efficient in the reduction of their average grain size which can be brought down to 5–10 nm in less than 3 h.

In this study, we subjected a brittle $SmCo_5$ alloy to successive dry and wet HEBM and discovered that the nanocrystalline structure acquired in the course of dry milling strongly influences the evolution of the particle shape during the second milling stage. The detailed characterization of the alloys subjected to this two-stage processing is included in this paper.

2. Experiment

Alloys with the nominal compositions $Sm_2(Co_{0.8}Fe_{0.2})_{17}$, $SmCo_5$ and $PrCo_5$ were prepared from pure components by arc-melting. In order to offset oxidation of the RE during milling, the $SmCo_5$ and $PrCo_5$ alloys were made with 2 extra at.% (relative) of the RE; also, the appropriate excess of Sm was added to compensate the evaporation loss of this element during melting. Prior to milling, which was performed at a ball-to-powder ratio of 8–10 using a Spex-8000M mill, the ingots had been crushed down to less than 300 μm. Dry HEBM was done under argon (after evacuating the milling vial to 10^{-3} Torr) for up to 240 min. An additional milling in ethanol for 5 min has been used to collect the powder stuck to the balls and to the vial interior during the dry milling; we do not include this 5 min in the nominal milling time count. Wet HEBM was performed in heptane for up to 720 min. The surfactant (oleic acid, OA), was added to heptane in the amount of 0–15 wt% of the powder mass. No washing/separation was employed when studying the wet-milled *nanoparticles*; the specimens were prepared by simply allowing the carrier liquid with suspended particles to dry. In contrast, when the evolution of particle shape was studied, the powders were washed successively in heptane and ethanol for at least three times. Some of the powders were additionally annealed for 30 min at 500–650 °C under argon.

The structure and morphology of the powders were characterized by transmission electron microscopy (TEM) with a JEOL JEM-3010 instrument, scanning electron microscopy (SEM) with a JEOL JSM-6335F instrument and x-ray diffraction (XRD) with a Philips diffractometer operating with Cu Kα radiation; the surface of the particles was studied by Fourier transform infrared (FTIR) spectroscopy with a Thermo Nicolet Nexus 670 instrument. All TEM studies were done on as-obtained particles, without thinning. The XRD data were processed with a Powder Cell program [31]; crystallite size and microstrain were estimated from the broadening of the XRD peaks using the Williamson–Hall plots [32] after correcting the XRD data for the Kα_2 contribution and instrumental broadening. For magnetic measurements, which were performed at room temperature with a vibrating sample
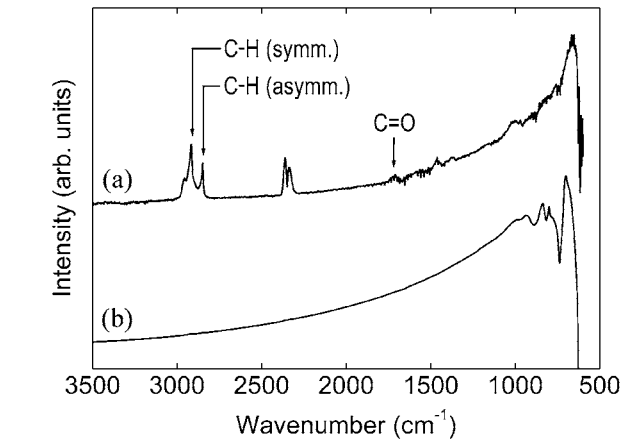

Figure 1. FTIR spectra of $PrCo_5$ powders milled for 60 min in heptane (a) with OA and (b) without OA.

magnetometer, the samples were immobilized with wax in the presence of a 19 kOe orienting field and, in the case of $SmCo_5$, additionally magnetized by a pulsed field of 100 kOe.

3. Fabrication of $Sm_2(Co, Fe)_{17}$, $SmCo_5$ and $PrCo_5$ nanoparticles via surfactant-assisted wet HEBM

Figure 1 compares the FTIR spectra of $PrCo_5$ samples milled with and without the addition of OA. The peaks at 2335–2360 cm^{-1} are believed to be caused by carbon dioxide present in the air. The peaks at 2922, 2853 and 1705 cm^{-1} correspond to the C–H (symmetric and asymmetric oscillations) and C=O bonds [33]. Importantly, the peak at 1705 cm^{-1} is dramatically suppressed compared to the spectrum of pure OA [33] indicating that the C=O bond is broken. Thus, one can suggest that, during the surfactant-assisted milling of the RE–Co powders, the OA molecule is attached to the particle in carboxylate form.

Surfactant-assisted milling of the $Sm_2(Co, Fe)_{17}$ alloy yielded highly uniform single-crystal particles 5–6 nm in size [18] shown in figure 2(a). The $SmCo_5$ and $PrCo_5$ alloys milled under similar conditions were less uniform (see figure 2(b)), and they exhibited a tendency to form what appears to be rod-shaped particles, especially for longer milling times. The formation of such rod-shaped nanoparticles was earlier explained [14] through either selective cleavage of crystals along the preferred orientation or anisotropic 'growth' of the nanoparticles. The selective cleavage mechanism, though possible, is expected to be more prominent at the *early* stage of milling. It is, therefore, more likely that the rod-shaped particles evolve through the anisotropic 'growth' mechanism. Because elemental diffusion through the carrier liquid is highly improbable, this growth must occur via coalescence of the smaller particles. Its anisotropy can be naturally explained by assuming that the coalescence is driven by the magnetostatic interaction between the single-domain particles.

The addition of OA to the carrier liquid is critical for obtaining the RE–Co nanoparticles [34]. Figure 3 compares the magnetic properties of field-oriented $PrCo_5$ powders wet-milled with and without the surfactant. The minimum
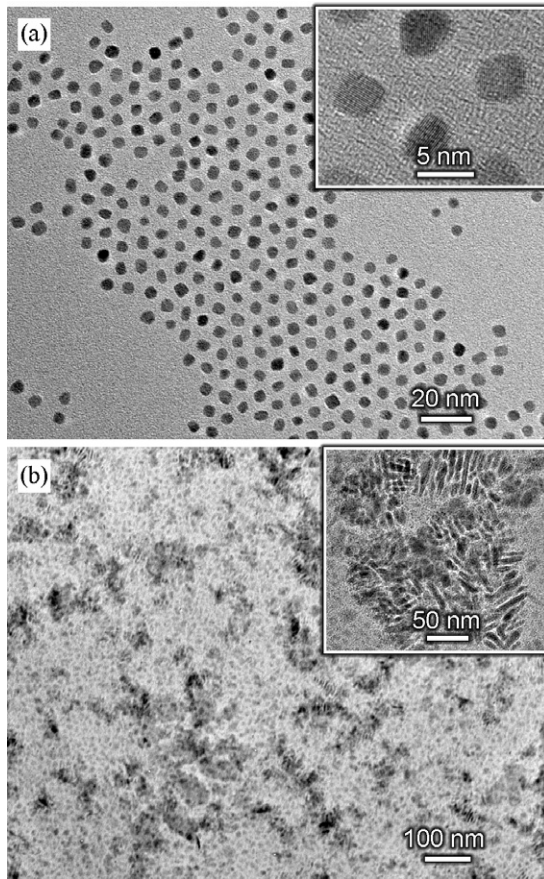
Figure 2. TEM images of Sm–Co nanoparticles obtained via surfactant-assisted wet milling: (a) $Sm_2(Co_{0.8}Fe_{0.2})_{17}$ milled for 240 min and (b) $SmCo_5$ milled for 720 min.

Figure 3. Remanent magnetization and intrinsic coercivity of $PrCo_5$ powders milled in heptane with and without additions of surfactant. Powders were magnetically oriented and the measurements were corrected for self-demagnetizing field.

Figure 4. XRD spectra for (a) isotropic and (b) field-oriented $PrCo_5$ powders after milling for 720 min in heptane in the presence of OA.

of remanence M_r and the maximum of coercive force H_c which the powders milled without OA exhibit after about 100 min must correspond to a polycrystalline state of the powder particles with mostly randomly oriented grains. The polycrystallinity during milling is usually being induced via coalescence of the particles and/or via the formation of new (sub)grains [35]. Further milling probably decreases the average grain size to values comparable to the effective exchange length, thus leading to the enhanced (isotropic) M_r and decreased H_c [36, 37]. The particles milled with OA exhibit much slower evolution of M_r and H_c, but their trend also appears to point toward increasing polycrystallinity. However, after 720 min of milling with OA, the $PrCo_5$ powders are still anisotropic, as can be seen in figure 4. The evolution of magnetic properties of the $PrCo_5$ and $SmCo_5$ powders with surfactant-assisted HEBM is very similar, though H_c of the latter reaches 19 kOe [18] because of the much higher magnetocrystalline anisotropy of the $SmCo_5$ compound.

4. Evolution of SmCo₅ particles throughout dry HEBM

As part of our experiment with successive dry and wet HEBM, we have done a detailed investigation of the milling of $SmCo_5$ alloy in argon. SEM characterization reveals a very rapid
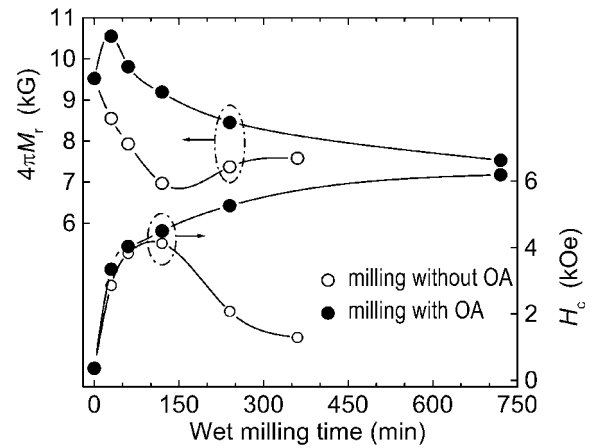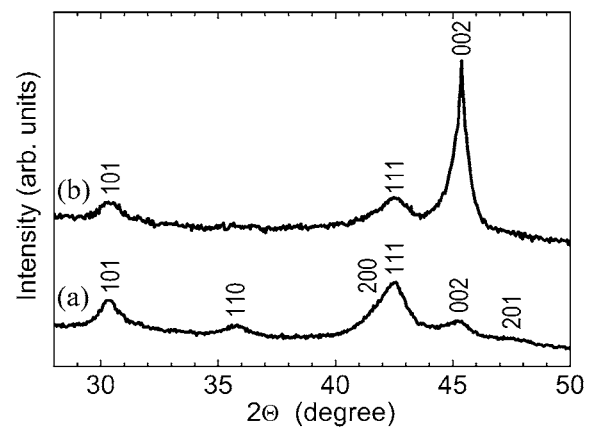
decline of the average particle size in the first minutes of the dry milling, as the cast material breaks up. Powders dry-milled for 1 min are shown in figure 5(a); they consist mostly of non-agglomerated particles 1–30 μm in size with characteristically polygonal shapes and sharp edges. After 5 min of milling, only a few separate particles with these features can still be found, as the smallest particles are being increasingly coalesced with each other and with the bigger particles. As shown in figures 5(b) and (d), the newly assembled particles (agglomerates) appear 'loose' and their size varies broadly from a few microns to tens of microns. After a prolonged milling, the assembled particles become denser and more uniform in size. The powders milled for 240 min (the longest milling time used in this study) shown in figures 5(c) and (e) consist of particles ranging from 6 to 10 μm. A qualitatively similar evolution of the $SmCo_5$ powder dry-milled with a different type of mill was reported in [38].

The structural properties of the dry-milled $SmCo_5$ alloy determined from broadening of the XRD peaks [32] and the corresponding hard magnetic properties are listed in table 1. The average crystallite size rapidly reaches the nanometer
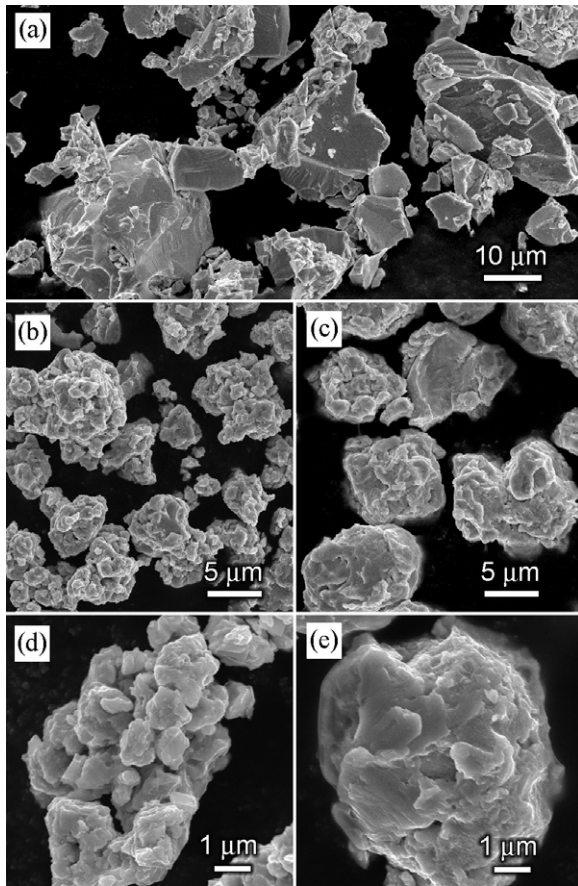
Figure 5. SEM images of dry-milled SmCo$_5$ alloy: powders milled for (a) 1 min, (b) 15 min and (c) 240 min; examples of (d) loosely and (e) densely cold-welded particles after milling for 45 and 240 min, respectively.

Table 1. Average crystallite size, microstrain, remanent magnetization M_r and intrinsic coercivity H_c of SmCo$_5$ alloy after dry milling in argon. Magnetization data were not corrected for self-demagnetizing field.

Milling time (min)	Crystallite size (nm)	Microstrain (%)	M_r (emu g^{-1})	H_c (kOe)
0	>5000	0.01	20.1	1.5
1	75.4	0.10	81.4	11.5
15	23.1	0.39	53.6	18.7
45	12.2	0.50	54.3	16.8
240	6.0	0.68	61.3	6.24

as enhancement of the saturation magnetization; in fact, the magnetizing field of 55 kOe used in [29] was not high enough to saturate the magnetization of the SmCo$_5$. Both the increase of remanence and decrease of coercivity must be expected in a nanocrystalline ferromagnet as the direct result of intergranular exchange coupling [36, 37]. Though local amorphization in the intergranular regions [29] is very likely, there are no sufficient reasons to consider an amorphous phase as the major factor leading to the decline of coercivity.

There is a clear qualitative similarity between the evolution of magnetic properties of the dry-milled SmCo$_5$ alloy and the PrCo$_5$ alloy wet-milled without the surfactant (figure 3). It appears that the same changes in the grain structure and particle morphology occur during dry milling at a rate six times the rate for surfactant-free wet milling.

5. Fabrication of SmCo$_5$ ultra-thin flakes via successive dry and wet HEBM

When the dry-milled SmCo$_5$ alloy had been subjected to a subsequent milling for 180 min in heptane in the presence of OA, the resulting powders were found to contain platelet-shaped particles, but their amount and morphology was strongly influenced by the duration of the preceding dry milling. The powder which had not been dry-milled at all or had been dry-milled for only 1 min exhibits a fairly complex morphology shown in figure 6(a). Most of the powder volume is made by elongated 'kebab-like' particles; a close-up of one such particle is shown in the inset. These particles, some of them tens of microns long, are assembled from platelet-shaped elements with an average thickness of 0.1–0.5 μm and an aspect ratio of 10–50. There are also a few stand-alone flakes. Since the precursor powder, which was not subjected to dry milling, did not contain agglomerated particles, we must conclude that the 'kebab-like' SmCo$_5$ particles resulted from an agglomeration process specific to surfactant-assisted wet milling. One can assume that, since a liquid environment, especially in the presence of surfactants, reduces the cold welding [19, 20], the ingot pieces had been flattened by a micro-forging process [39, 40] before they became assembled into the loose 'kebab-like' agglomerates.

When the precursor powders were dry-milled for 15 min or longer, the solvent after wet milling remained clear. Figure 6(b) shows the result of wet milling after dry milling for 15 min. The powder is highly inhomogeneous with many small fragments and irregularly shaped agglomerates.

range and, after 15 min, tends to saturate. After 240 min, the average crystallite size is found to be 6 nm. The microstrain also changes most rapidly during the first 15 min of milling, but its tendency towards saturation is less pronounced than that of its crystallite size. This result differs somewhat from the one reported in [29], where XRD peak broadening was analyzed with a different technique and the microstrain exhibited a nearly linear increase with milling time. The remanent magnetization reaches its maximum value after 1 min of dry milling, when break-up of the ingot already occurred, but without significant agglomeration of the particles or misorientation of the newly formed nanograins [35]. After milling for 15 min, when the coercivity reaches its maximum value, presumably at the optimum combination of the average grain size and microstrain, the remanence of the field-oriented powder declines to the value which is expected for a polycrystalline material with randomly oriented uniaxially anisotropic non-interacting grains. With more prolonged dry milling the remanence increases again, whereas the coercivity decreases. In [30], a similar remanence enhancement in HEBM PrCo$_5$ was attributed to intergranular exchange coupling, whereas the decline of coercivity was explained as the result of amorphization. In the case of HEBM SmCo$_5$ [29], a remanence enhancement was also observed, but misinterpreted
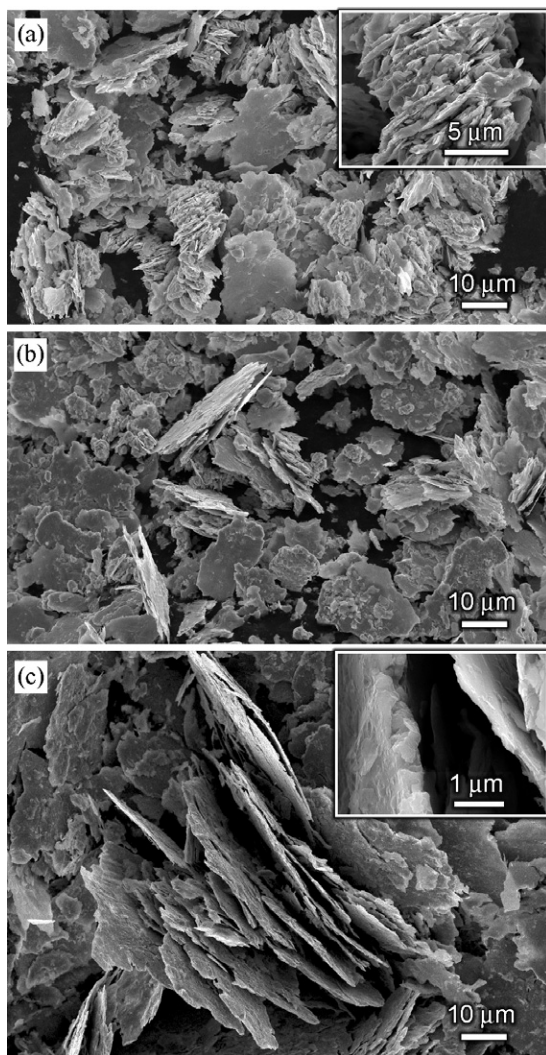
Figure 6. SEM images of SmCo$_5$ alloy after surfactant-assisted wet milling for 180 min preceded by dry milling for (a) 0 min, (b) 15 min and (c) 240 min.

Figure 7. TEM images of SmCo$_5$ flakes after surfactant-assisted wet milling for 180 min which was preceded by dry milling for 240 min: (a) as-milled and (b) annealed for 30 min at 650 °C.

However, most of the particles are now shaped as platelets. The absence of nanoparticles small enough to be suspended in the solvent and the increased average aspect ratio of the particles may indicate that the material becomes more malleable. This probable change in the mechanical properties correlates well with the reduction of the average crystallite size (see table 1). It has been suggested [35] that the mechanical properties of nanocrystalline materials prepared by mechanical attrition are no longer controlled by dislocation movement through the crystals (or by lack of such movement, as with the brittle SmCo$_5$) but by cohesion across the grain boundaries. Amorphous inter-crystalline regions which were believed to be formed in the HEBM SmCo$_5$ [29] must greatly facilitate the grain-boundary sliding.

Dry milling of the precursor for 240 min led to a wet-milled SmCo$_5$ powder consisting of uniform flakes with a thickness of 100–500 nm and a lateral size up to 50 μm. The typical morphology of these flakes is shown in figure 6(c). The flakes must have evolved from the 'dense' assembled particles like the one shown in figure 5(e). The rough estimate
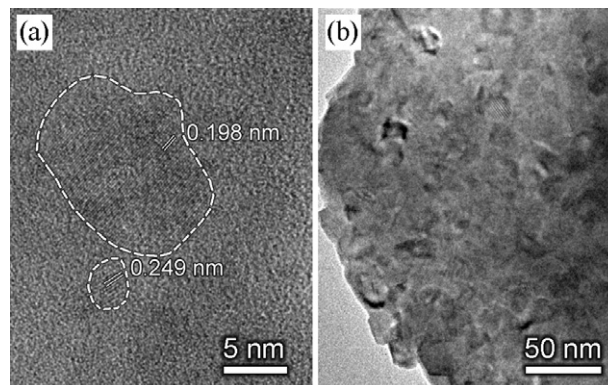
of average volume of the precursor particles (300 μm^3) is reasonably close to the volume of the typical flake (e.g. 35 μm × 35 μm × 0.25 μm), indicating that little, if any, coalescence or breaking of the particles had taken place during the wet milling. Thus, the evolution of particle shape for the nominally brittle SmCo$_5$ alloy wet-milled after prolonged dry milling is similar to that of ductile materials [23–26]. This result is perfectly consistent with the above model of nanostructure-induced ductility. It should be noted, however, that unlike at least some of the truly ductile materials, which reportedly may evolve into flakes while being wet-milled without added surfactants [23, 24], the nanocrystalline SmCo$_5$ powders milled in heptane *without* OA do not contain any flakes. Moreover, they exhibit a markedly broadened particle size distribution compared to the dry-milled precursors; this can only result from a considerable cold welding and breaking of the particles. We still have to find the critical concentration of the surfactant; the powders milled with 7.5 wt% OA were found to have a morphology very similar to that for 15 wt%.

According to the XRD peak broadening analysis, the wet milling reduces further the average crystallite size of the powder dry-milled for 240 min, from 6 to approximately 5.2 nm. The lattice parameters of the SmCo$_5$ phase ($a = 0.4995$, $c = 0.4042$ nm) suggest that the phase is slightly enriched with Co compared to the stoichiometric compound ($a = 0.5004$ nm, $c = 0.3969$ nm). Some of the SmCo$_{5+\delta}$ crystallites can be seen in the high-resolution TEM image presented in figure 7(a): the lattice spacing values of 0.198 and 0.249 nm correspond to the (002) and (110) planes, respectively.

The magnetic properties of SmCo$_5$ flakes are very close to those of their precursor powders and, as we have discussed before, are associated with extremely small grain sizes. Table 2 presents the crystalline and magnetic properties of the flake subjected to a re-crystallization annealing. The annealing increases the average crystallite size and decreases the microstrain of the SmCo$_{5+\delta}$ phase and also produces a new Sm$_2$O$_3$ phase. The average grain size of the SmCo$_{5+\delta}$ phase, 16.4 nm, is in good agreement with the TEM data presented in figure 7(b). The changes of the average grain size and microstrain must be the reason for the decreased M_r and

Table 2. Structural properties of $SmCo_{5+\delta}$ phase and intrinsic coercivity H_c of as-milled and annealed $SmCo_5$ flakes (dry milling for 240 min was followed by wet milling for 180 min). Phases were determined by XRD.

Annealing temperature (°C)	Phases	Crystallite size[a] (nm)	Microstrain[a] (%)	H_c^a (kOe)	H_c^b (kOe)
No	$SmCo_{5+\delta}$	5.2	0.95	6.2	5.6
500	$SmCo_{5+\delta}$, Sm_2O_3	7.9	0.56	12.3	14.7
650	$SmCo_{5+\delta}$, Sm_2O_3	16.4	0.26	16.9	19.0

[a] Wet milling with 15 wt% OA.

[b] Wet milling with 7.5 wt% OA.

increased H_c. Note that the higher coercivity can be attained if a lesser amount of OA had been used.

6. Conclusions

High-energy ball milling, which for two decades has been used for the manufacturing of nanocrystalline and amorphous RE–TM permanent magnet materials, has also considerable potential in the fabrication of submicron and nanometer RE–TM powders with specific particle sizes and shape. The particle morphology can be effectively controlled via the milling mode (dry, wet or surfactant-assisted wet milling). Single-crystal nanoparticles produced by the surfactant-assisted wet HEBM and submicron-thin polycrystalline flakes obtained via the combination of dry and surfactant-assisted wet HEBM may serve as a hard magnetic component in the synthesis of long-expected nanocomposite magnets. The possible applications of the hard magnetic flakes also include laminated magnets with increased electrical resistivity and high-gradient magnetic filters. Finally, the method we developed for fabrication of the RE–TM flakes may allow manufacturing of ultra-thin flakes from other brittle materials.

Acknowledgments

References

[1] Skomski R and Coey J M D 1993 *Phys. Rev.* B **48** 15812
[2] Zeng H, Li J, Liu J P, Wang Z L and Sun S 2002 *Nature* **420** 395
[3] Töpfer J and Pawlowski B 2004 *J. Magn. Magn. Mater.* **272–276** e1867
[4] Zhang J, Evans P and Zangari G 2004 *J. Magn. Magn. Mater.* **283** 89
[5] Wan H and Berkowitz A E 1995 *Scr. Metall. Mater.* **32** 1827
[6] Hansen M F, Vecchio K S, Parker F T, Spada F E and Berkowitz A E 2003 *Appl. Phys. Lett.* **82** 1574
[7] Tang Y J, Parker F T, Harper H, Berkowitz A E, Vecchio K, Rohatgi A and Ma B M 2005 *Appl. Phys. Lett.* **86** 122507
[8] Ram S 1997 *J. Mater. Sci.* **32** 4133
[9] Lee J I, Kwon H W and Kang Y S 2008 *J. Magn.* **13** 102
[10] Liu W and McCormick P G 1999 *Nanostruct. Mater.* **12** 187
[11] Liu W and McCormick P G 1999 *J. Magn. Magn. Mater.* **195** L279
[12] Kirkpatrick E M, Majetich S A and McHenry M E 1996 *IEEE Trans. Magn.* **32** 4502
[13] Majetich S A and Kirkpatrick E M 1997 *IEEE Trans. Magn.* **33** 3721
[14] Chakka V M, Altuncevahir B, Jin Z Q, Li Y and Liu J P 2006 *J. Appl. Phys.* **99** 08E912
[15] Cha H G, Kim Y H, Kim C W, Kwon H W and Kang Y S 2007 *J. Phys. Chem.* C **111** 1219
[16] Wang Y P, Li Y, Rong C B and Liu J P 2007 *Nanotechnology* **18** 465701
[17] Yue M, Wang Y P, Poudyal N, Rong C B and Liu J P 2009 *J. Appl. Phys.* **105** 07A708
[18] Akdogan N G, Hadjipanayis G C and Sellmyer D J 2009 *J. Appl. Phys.* **105** 07A710
[19] Somasundaran P and Lin I J 1972 *Indust. Eng. Chem. Process Des. Dev.* **11** 321
[20] Guérard D 2008 *Rev. Adv. Mater. Sci.* **18** 225
[21] Kaczmarek W A and Ninham B W 1995 *Mater. Chem. Phys.* **40** 21
[22] Berkowitz A E, Lahut J A, Jacobs I S, Levinson L M and Forester D W 1975 *Phys. Rev. Lett.* **34** 594
[23] Zhou P H, Deng L J, Xie J L and Liang D F 2008 *J. Alloys Compounds* **448** 303
[24] Kao S T and Dun J G 2004 *J. Electron. Mater.* **33** 1445
[25] Wang X, Gong R Z, Li P G, Liu L G and Cheng W M 2007 *Mater. Sci. Eng.* A **466** 178
[26] Xiao X, Zeng Z G, Zhao Z W and Xiao S W 2008 *Mater. Sci. Eng.* A **475** 166
[27] Radlinski A P, Calka A, Ninham B W and Kaczmarek W A 1991 *Mater. Sci. Eng.* A **134** 1346
[28] Jiang B and Weng G J 2004 *Int. J. Plast.* **20** 2007
[29] Leslie-Pelecky D L and Schalek R L 1999 *Phys. Rev.* B **59** 457
[30] Chen Z M, Meng-Burany X and Hadjipanayis G C 1999 *Appl. Phys. Lett.* **75** 3165
[31] Kraus W and Nolze G 1996 *J. Appl. Crystallogr.* **29** 301
[32] Williamson G K and Hall W H 1953 *Acta Metall.* **1** 22
[33] Jain T K, Morales M A, Sahoo S K, Leslie-Pelecky D L and Labhasetwar V 2005 *Mol. Pharmacol.* **2** 194
[34] Akdogan N G, Hadjipanayis G C and Sellmyer D J 2009 *IEEE Trans. Magn.* **45** 4417
[35] Fecht H J 1995 *Nanostruct. Mater.* **6** 33
[36] Herzer G 1990 *IEEE Trans. Magn.* **26** 1397
[37] Skomski R 2003 *J. Phys.: Condens. Matter* **15** R841
[38] Kahn M L, Bobet J L, Weill F and Chevalier B 2002 *J. Alloys Compounds* **334** 285
[39] Benjamin J S and Volin T E 1974 *Metall. Trans.* **5** 1929
[40] Suryanarayana C 2001 *Prog. Mater. Sci.* **46** 1